Distribution of straight-chain lengths in unannealed and annealed solution-crystallized polyethylene by Raman spectroscopy

R. G. Snyder
Department of Chemistry, University of California, Berkely, CA 94720, *USA*

and J. R. Scherer
Western Regional Research Center, Science and Education Administration, US Department of Agriculture, Berkeley, CA 94716, *USA*

and D. H. Reneker and J. P. Colson
Center for Materials Science, National Bureau of Standards, Washington, DC 20234, *USA*
(*Received* 20 *January* 1982)

The effect of annealing on the morphology of solution-crystallized polyethylene has been studied by analysing the shape of the low-frequency Raman LAM-1 band. The distributions of lengths of straight-chain segments have been determined for samples annealed at different temperatures. Unannealed samples, which have distribution peaks L_{max} near 100 Å, have halfwidths $\Delta L_{1/2}$ less than 20 Å. However, this narrow distribution is drastically broadened when the sample is annealed. The broadening is less if the breadth of the distribution of the unannealed sample is initially less. For equilibrium crystallized samples, the observed halfwidth and peak position of LAM-1 are found to be related. This relation can be understood quantitatively if it is assumed that $\Delta L_{1/2}$ and L_{max}^{-1} are linearly related as is indeed found to be the case for solution-crystallized samples. As L_{max}^{-1} becomes very large, $\Delta L_{1/2}$ approaches a limiting value near 300 Å.

Keywords Polyethylene; LAM; Raman spectroscopy; lamellar crystals; stem length; lamellar thickness

INTRODUCTION

Few, if any, polymer systems have been subjected to a greater number of investigations by a greater variety of structural methods than has solution-crystallized polyethylene. The existence of a lamellar structure consisting largely of planar zigzag segments of the molecule is now firmly established. Important areas of current interest are concerned with how the straight-chain segments within the crystal are interconnected, the conformational nature of the material that is not included in planar zigzag segments, and how annealing affects the structure. Two new physical techniques have been recently applied to these problems: neutron scattering, which measures the radius of gyration and thereby provides information on the trajectory of a polymer chain in the crystal[1], and low-frequency Raman spectroscopy, which provides information on the lengths of the planar zigzag segments[2,3].

We report here on a low-frequency Raman study of solution-crystallized polyethylene in which this technique is used to determine the distribution of lengths of planar zigzag segments, often referred to in this paper as the 'distribution of straight-chain segments' or simply as the 'distribution'. The study reveals unexpected and drastic changes in the straight-chain length distribution that occur as a result of annealing. A description of these changes and their concomitant structural implications comprise most of this presentation.

METHOD

The spectroscopic method used is based on an analysis of the shape of the LAM-1 band, the lowest-frequency and most intense band in the progression of Raman-active longitudinal-acoustic modes (LAM-k, $k = 1, 3, 5 \ldots$). The first few members of this progression appear at low frequencies in the Raman spectra of many crystalline polymers. The frequency ν (cm^{-1}) of LAM-1 for an isolated straight chain whose length L (Angstroms) is much larger than bond distances is given by

$$\nu = aL^{-1} \quad (1)$$

where a is a constant. This relation has been verified experimentally for LAM-1 modes of long crystalline n-alkanes[4] and for polymers[2,5] in those cases where lamellar thicknesses were available from low-angle X-ray scattering measurements. For polyethylene, a is approximately[2] 3093 in the units employed in equation (1).

0032-3861/82/091286-09$03.00

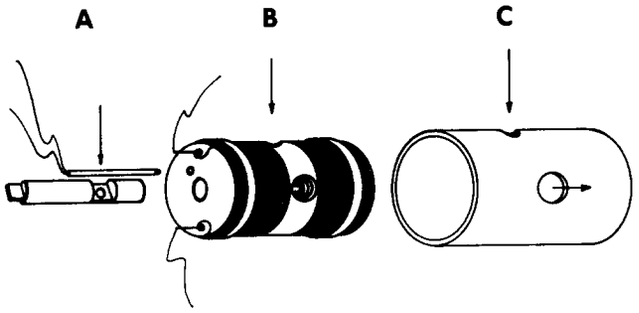

Figure 1 Schematic diagram of Raman-cell heating-oven used to anneal samples *in situ*. A. Cu/constantan thermocouple in a 1 mm diameter ceramic tube; sample holder: 3 mm diameter stainless steel rod with a 15 mm diameter hole into which the sample is pressed. B. Furnace: 1.25 cm diameter aluminum rod, 3.75 cm long, with holes for sample holder and thermocouple. The outside of the rod is wrapped with glass-insulated manganin wire (34 ga, 7.25 ohms/ft, 100 ohms total resistance). An asbestos spacer over the winding at both ends provides a tight fit between the furnace and the pyrex tube shield (14 mm ID) shown at C. The furnace and shield have holes for focusing the laser beam (downward arrows) on the sample and for collecting the 90° scattered light

Equation (1) can be used to estimate lamellar thickness from the observed frequency of the LAM-1 band. There is a difficulty, however, in that the lamellae found in most samples are not uniform in thickness. Evidence for a significant variation in thickness comes from a variety of sources: electron-microscopic studies of fracture surfaces[6,7]; small-angle[8] and wide-angle[9,10] X-ray line shape analysis; melting point distribution[11]; selective degradation studies of fold surfaces[12,13]. Because there is a distribution of lengths of straight-chain segments constituting the crystalline core of the lamellae, band halfwidths (band width at half peak-height) of LAM-1 for crystalline polyethylene are significantly broader than those of a crystalline n-alkane whose extended-chain length is comparable with the lamellar thickness of the polymer crystal. One effect of this broadening is to displace the observed maximum of LAM-1 away from the frequency that corresponds to the most likely straight-chain length. If the distribution is broad, this displacement can be large[14] so that equation (1) cannot be used to determine the most probable length.

The band shape observed for LAM-1 after correction for the finite resolution of the spectrometer is determined both by the presence of a length distribution and by the 'natural' band shape, i.e., by the band shape of the LAM-1 associated with a crystal whose chains all have the same length. The natural band shape is determined by intra- and intermolecular relaxation processes that are at present not well understood. In the case of samples that are highly disordered such as drawn polyethylene, the width of the LAM-1 band is large and is essentially determined by the straight-chain length distribution alone[3]. However, for unannealed solution-crystallized samples, the observed band width is comparable with the natural line width so that some correction is necessary.

The assertion that for polyethylene most, if not virtually all, of the breadth of LAM-1 in excess of the 'natural' width is to be attributed to a distribution of lengths of straight-chain segments, finds support from both spectroscopic and nonspectroscopic studies. The halfwidth and dissymmetry of the distributions determined from Raman spectra are, within experimental error, in complete accord with the independent findings of the nonspectroscopic techniques cited earlier. Spectroscopic evidence based on a comparison of the theoretical and experimental relations between the frequencies, intensities, and halfwidths of LAM-1 and LAM-3 bands of polyethylene demonstrates the presence of a distribution of lengths of straight-chain segments and indicates that these segments are, to a good approximation, noninteracting vibrational systems[2].

The distribution $f(L)$ of lengths of straight-chain segments is related to the shape of the LAM-1 band through the expression

$$f(L) = Av^2 B_v I_v^{obs} \tag{2}$$

where A is a constant, I_v^{obs} is the Raman intensity observed at frequency v, and $B_v = 1 - \exp(-hcv/kT)$ where T is the temperature of the sample[2].

EXPERIMENTAL

Spectra were measured using a Spex 1401 double monochromator with an RCA 31034A photomultiplier*. Stray light was reduced by tuning an etalon in an Argon ion laser (5145 Å) to excite a single longitudinal mode which coincides in frequency with an absorption line of I_2 vapour at 80°C[15]. The gas cell (10 cm path length) containing I_2 vapour was positioned between the light-collection optics and the entrance slit of the monochromator. Removal of I_2 absorption lines from the Raman spectrum was accomplished by ratioing, at each frequency where a measurement was made, the intensity of the observed Raman spectrum with the intensity of a white light absorption spectrum of I_2, the latter spectrum being obtained through the same absorption cell used to filter the Raman scattering[16]. The power level of the tuned laser was between 200 and 250 MW.

To be able to quantitatively compare Raman intensities for a given sample before and after annealing, we used a special Raman scattering cell which served as both the sample holder and the annealing oven. This made it possible to anneal a sample without removing it from the spectrometer thereby ensuring that the same part of the sample was always being observed. *Figure* 1 shows a schematic diagram of the oven. It consists of a 12.7 mm diameter aluminum cylinder wrapped with insulated heater wire and bored to accept a stainless steel sample holder and thermocouples, and to allow entrance for the focused laser beam and exit for the 90° scattered radiation. The heater wire and one of the two thermocouples are attached to an RFL-1 proportional controller. The second thermocouple is connected to an independent read-out device. The thermocouples were positioned to within 1 mm of the sample and the temperature at this point was regulated to within 0.2°C.

Three samples of solution-crystallized polyethylene were prepared by the self-seeding method[17]. A dilute solution (0.1 percent) of the polymer dissolved in tetrachloroethylene at 120°C was cooled to 70°C, then the temperature was raised and held at 90°C for one to two hours to dissolve most of the precipitate leaving only

* Reference to a company and/or product is only for purposes of information and does not imply approval or recommendation of the product by the Department of Agriculture or the National Bureau of Standards to the exclusion of others which may also be suitable

Table 1 Data on the solution-crystallized polyethylene samples used in this study

Sample	Origin (SRM Number[a])	M_w	M_n	L_{SAXS}(Å)[b]
I	1475	55 400	18 400	115
II	1484	119 600	100 500	106
III	1475	55 400	18 400	108

[a] SRM numbers refer to National Bureau of Standards 'Standard Reference Material' samples
[b] Unannealed

invisible seed crystals, and finally returned to 70°C for isothermal crystallization. The crystallization times for samples I and II were about 18 h, and for sample III about 340 h. Samples I and II were pressed to form translucent films which typically are birefringent. Sample III, which was not pressed, was a porous highly crystalline, highly-scattering solid. Other relevant information about these samples is given in *Table* 1. The effects of different types of fold domains[18] which may be present in these crystals is not discussed in this paper.

RESULTS

Unannealed samples

Low-frequency Raman spectra of samples I, II, and III are shown in *Figure* 2. Small-angle X-ray scattering (SAXS) measurements on these samples yield interlammelar spacings of 115, 106, and 108 Å which may be compared with straight-chain lengths 110, 106, and 127 Å derived from the observed frequencies of LAM-1 using equation (1). Part of the difference between the SAXS and LAM values may be the result of the straight-chain segments being tilted with respect to a normal to the crystal surface. This would have the effect of decreasing the SAXS derived value of L relative to that derived from LAM-1[19,20]. The observed half-widths of LAM-1 for samples, I, II, and III are respectively 7.2, 6.8, and 5.0 cm^{-1}.

As mentioned earlier, the distribution curve $f(L)$ is calculated from the shape of LAM-1, but only after the latter has been corrected for the convolution resulting from the finite width of the individual LAM-1 bands that comprise the LAM-1 band observed for the polymer. For most samples, this correction is small and can be ignored, and the observed shape can be used directly. However, this is not the case for unannealed samples. The bandwidth of LAM-1 for the unannealed sample is only about a factor of two larger than that of LAM-1 of a crystalline n-alkane whose chain length is comparable with the average stem-length of the polymer[2]. Consequently, the shape of LAM-1 of the polymer must be corrected since the distribution of lengths of straight-chain segments is responsible for only about half the observed width.

In principle, the true shape of the LAM-1 band could be recovered by deconvoluting with the 'natural' band shape derived from an n-alkane. In practice such a deconvolution calculation leads to an acceptably accurate band shape only in circumstances where spectra can be measured with much greater accuracy than was possible in the present case.

There is, however, a simple way of estimating the shape and halfwidth of the distribution based on the fact that both the LAM-1 band of the unannealed polymer and the LAM-1 band of a long crystalline n-alkane have shapes that are nearly Lorentzian. In that case, it turns out that the true band shape is also approximately Lorentzian[21]. We will now consider the observed band shape of LAM-1 of the unannealed polymer and that of the crystalline n-alkane n-$C_{94}H_{190}$. The latter, we will assume, represents to a good approximation the shape of the individual LAM-1 bands associated with straight-chain segments in the unannealed polymer sample.

The observed shape of LAM-1 for sample I is plotted in *Figure* 3 in terms of I_ν^α. The latter, which is defined

$$I_\nu^\alpha = C\nu B_\nu I_\nu^{obs}, \tag{3}$$

where C is a constant, is a more appropriate function to use than I_ν^{obs}, since it is temperature and frequency independent[14,22]. In *Figure* 3, the shape of LAM-1 for polyethylene crystals is compared with calculated Gaussian and Lorentzian line shapes, each of which have the halfwidth of the observed band. The calculated and observed curves are nearly indistinguishable except in the wings where the Lorentzian line clearly gives a better fit to the observed band. We note that the observed band is not quite symmetric, the high frequency wing being somewhat more intense than the low.

The n-alkane n-$C_{94}H_{190}$ has a length comparable to the length of a straight-chain segment in an unannealed sample. Measurements on n-$C_{94}H_{190}$ show that its LAM-1 band is similar in shape to LAM-1 for the polymer and, when expressed in terms of I_ν^α, is found to be significantly more Lorentzian than Gaussian, again by virtue of a better fit in the wings. As in the case of the polymer, the high frequency wing of LAM-1 is more intense than the low.

We can conclude that the true shape of LAM-1 of the unannealed sample is approximately Lorentzian. The true halfwidth $\Delta\nu_{\frac{1}{2}}^t$ of this band can be estimated from the following expression written here in a generalized form

$$(\Delta\nu_{\frac{1}{2}}^t)^n = (\Delta\nu_{\frac{1}{2}}^u)^n - d(\Delta\nu_{\frac{1}{2}}^s)^n \tag{4}$$

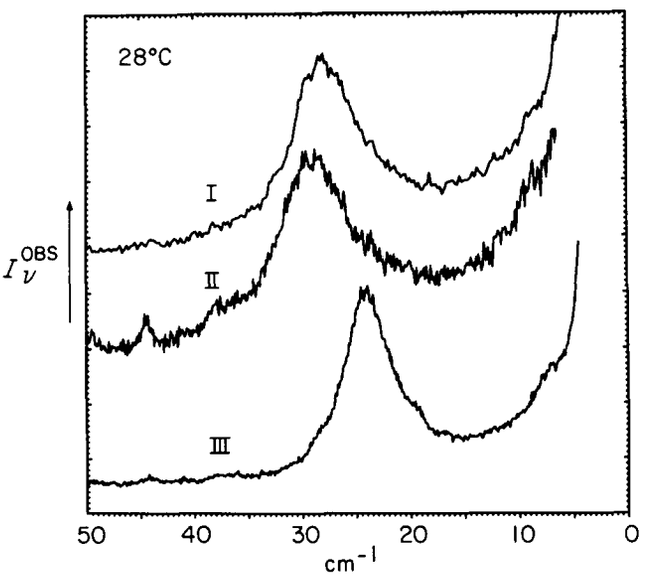

Figure 2 Low-frequency Raman spectra of unannealed solution-crystallized polyethylene: samples I, II, and III

where $\Delta\nu_{\frac{1}{2}}^{a}$ is the observed (apparent) halfwidth and $\Delta\nu_{\frac{1}{2}}^{s}$ is the halfwidth of the convoluting function, in the present case the band shape of LAM-1 of n-$C_{94}H_{190}$. The values of n and d depend on the shapes of the convoluted band and convoluting function and are listed in *Table* 2 for some specific cases. When all bands are Lorentzian $n=d=1$ so that $\Delta\nu_{\frac{1}{2}}^{i}=\Delta\nu_{\frac{1}{2}}^{a}-\Delta\nu_{\frac{1}{2}}^{s}$, i.e., the true halfwidth is just the difference between the observed halfwidths (slit corrected) of LAM-1 of the polymer and the n-alkane n-$C_{94}H_{190}$.

Our measured halfwidth for LAM-1 of n-$C_{94}H_{190}$ at room temperature is 3.4 cm^{-1}. An independent measurement in another laboratory gave a somewhat smaller value, 2.8 cm^{-1} [24]. We note that polymorphism in this sample may slightly affect the shape of the LAM-1 band[20]. The observed halfwidths must be corrected for the effect of the spectrometer slit width (1 cm^{-1}). For this, we assumed a triangular slit distribution function and used equation (4) with values for the parameters taken from *Table* 2 (case 4, ref. 23). After correction for slit effects, the halfwidths are 3.1 and 2.4 cm^{-1}, respectively, and these values were used to compute the halfwidths of the straight-chain length distributions given in *Table* 3. The halfwidths of the distributions are all less than 20 Å.

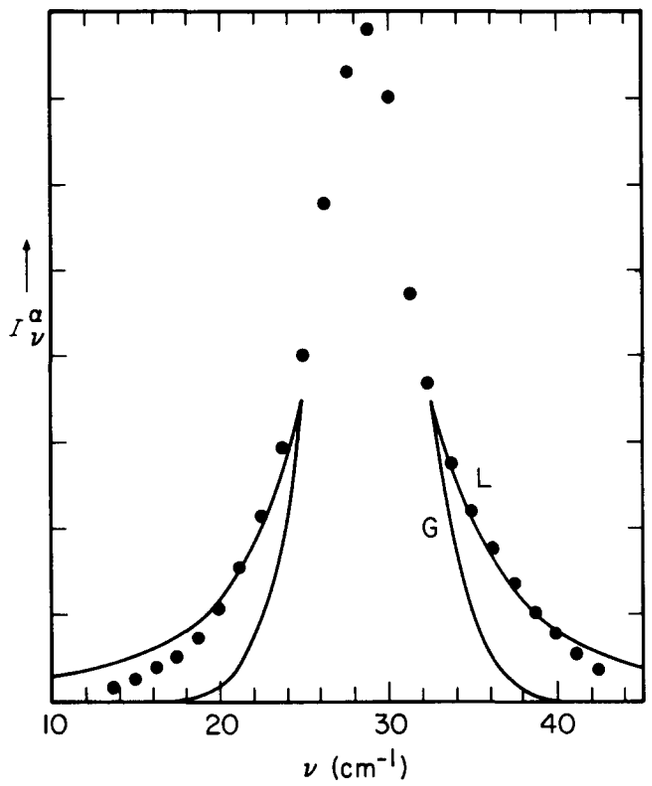

Figure 3 LAM-1 for unannealed sample I at 28°C (expressed in terms of scattering activity I_ν^α). The Gaussian (G) and Lorentzian (L) bands were computed using the peak height and halfwidth of the observed LAM-1 band

Annealed samples

In order that Raman intensities, and hence distributions, could be compared directly, annealing was carried out, in so far as possible, without disturbing the position of the sample in the spectrometer. After measuring its room temperature spectrum, the sample was annealed in air in the oven described previously, then cooled and remeasured. This cycle was repeated at successively higher annealing temperatures.

The accuracy of our measurements may be affected deleteriously, if, during the annealing, the sample moves or the optical properties of the sample change so as to modify the effective Raman scattering volume. We performed the following tests to monitor the accuracy of the measurements.

Firstly, we annealed a sample at 129°C for 1 h and measured its spectrum at room temperature. After the same sample was further annealed at 121°C for 4 h, its spectrum was remeasured. Annealing the sample a second time at a lower temperature would be expected to have little effect on the morphology so that differences between the two spectra reflect experimental reproducibility. The two spectra were found to be essentially identical.

A second kind of check on the accuracy of the experiments is possible if, as is reasonable in these highly crystalline samples, the total amount of material in the straight-chain segments remains essentially unchanged after annealing. In that case, the integrated intensity of the LAM-1 band

$$I=\int I_\nu^{obs}\,d\nu \qquad (5)$$

should remain nearly constant[14]. This was found to be the case for the pressed samples (I and II) but not for the unpressed (III). Annealing the unpressed sample resulted in a large increase in the integrated intensity associated with LAM-1 as may be seen in *Figure* 4. The increase in

Table 2 Coefficients for equation (3) of text relating true and apparent band halfwidths

	Band shape				
Case	Apparent	Convoluting	n	d	ref.
1	Lorentzian	Lorentzian	1	1	21
2	Gaussian	Gaussian	2	1	21
3	Lorentzian	Gaussian	2	2	23
4	Lorentzian	Triangular	2	2	23

Table 3 Halfwidths $\Delta L_{1/2}$ of the straight-chain length distributions for unannealed samples based on two different values for $\Delta\nu_{1/2}^{obs}$ of the LAM-1 band of n-$C_{94}H_{190}$: column a is for 3.4 cm^{-1} and b is for 2.8 cm^{-1}

Sample	ν (cm^{-1})	$\Delta\nu_{1/2}^{obs}$ (cm^{-1})	$\Delta\nu_{1/2}^{corr}$ (cm^{-1})	L_{max} (Å)	$\Delta L_{1/2}$ (Å)	
					a	b
I	28.0	7.2	7.2	110	16	19
II	29.2	6.8	6.65	106	13	15
III	24.4	5.2	5.0	127	10	14

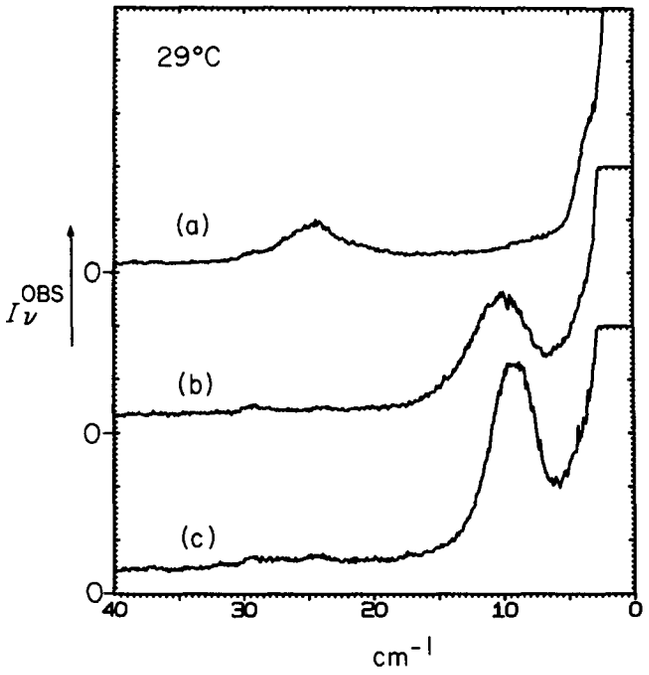

Figure 4 Low-frequency Raman spectra of sample III at 29°C: (a) unannealed; (b) annealed 65 min at 129°C; (c) annealed, in addition, 5 h at 132°C

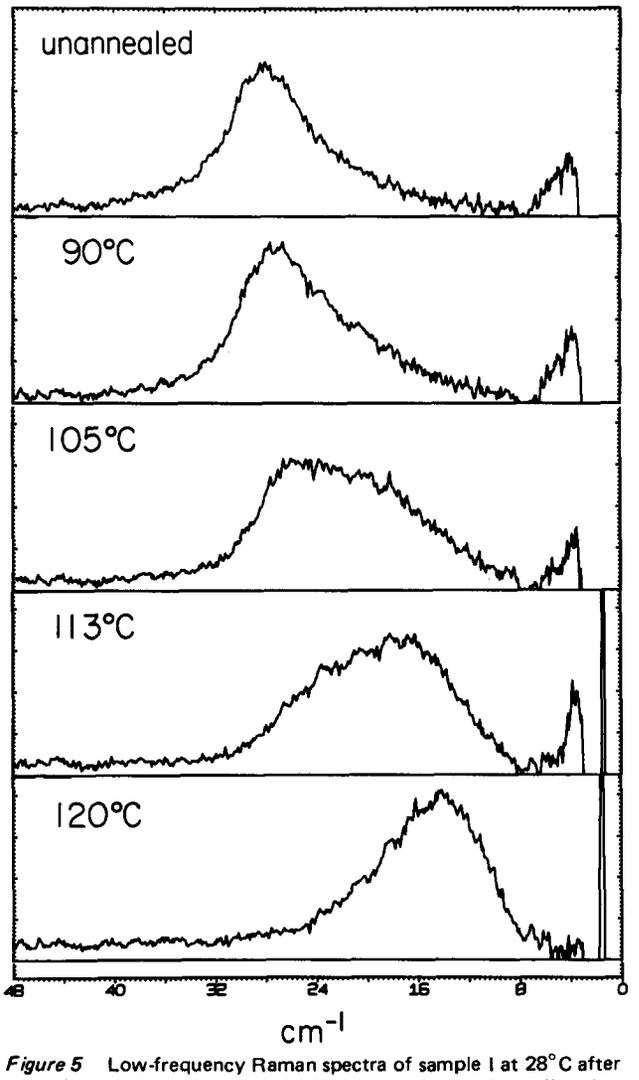

Figure 5 Low-frequency Raman spectra of sample I at 28°C after being annealed at successively higher temperatures. Annealing time at each temperature was 6 h

intensity as a result of annealing may be caused by changes in the packing of the lamellae in the sample so that the Raman-scattering sample volume is effectively increased.

The effect of annealing was studied systematically for sample I over the temperature range 90° to 120°C. The sample was annealed successively for 6 h at 90°, 105°, 113°, and 120°C, and Raman spectra were measured before and after each treatment. The spectra, corrected for background scattering, are shown in *Figure* 5.

The LAM-1 band changes its shape in a complex way as the sample is annealed at higher temperatures. For the annealed sample, the band is asymmetric. It is more intense on the low-frequency side of the band maximum. After the sample was annealed at 120°C, the asymmetry is reversed so that the band is now more intense on the high-frequency side. Bands associated with intermediate annealing temperatures appear to have shoulders. The distributions of straight-chain lengths derived from the spectra of *Figure* 5 have shapes (see *Figure* 6) that are markedly different from the spectra from which they were derived. The distribution curves change shape in a less complex way than their parent spectra.

DISCUSSION

Conservation of straight-chain length

We can now show that annealing the solution-crystallized sample does not appreciably affect the total length of straight-chain segments. For this purpose it is useful to define another distribution, $f(CH_2)$, which gives the total number of methylene groups associated with straight-chain segments of a particular length L. This distribution is related to $f(L)$ through

$$f(CH_2) \propto L f(L). \tag{6}$$

The total length of all straight-chain segments is given by the integral $\int f(CH_2)\,dL$. The distributions $f(CH_2)$ for sample I before annealing and after annealing at 120°C for

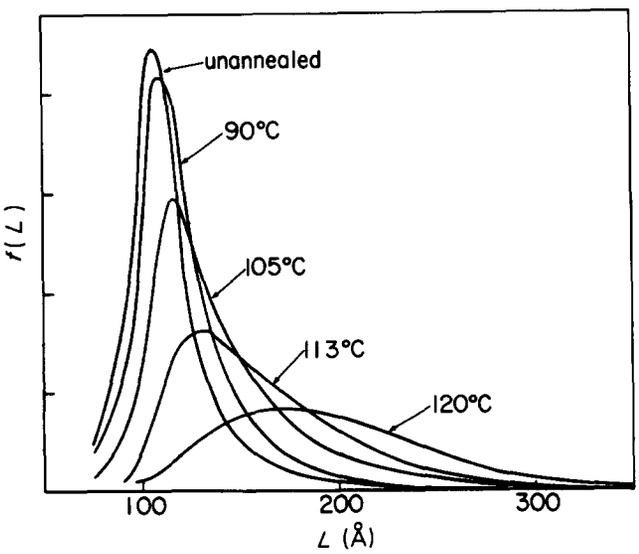

Figure 6 Chain-length distribution curves for sample I based on the spectra shown in *Figure 5*. Annealing temperatures are shown

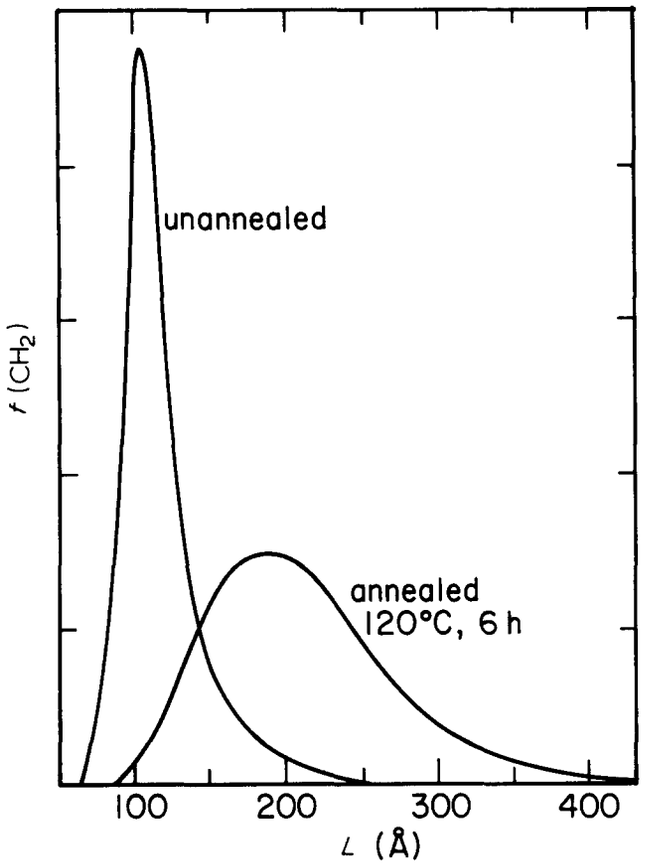

Figure 7 Distribution $f(CH_2)$ (total number of methylenes in all straight-chain segments of length L) for unannealed and annealed sample. Ratio of areas under distribution: unannealed/annealed = 0.90

6 h are shown in *Figure* 7*. The ratio of areas under $f(CH_2)$, unannealed to annealed, is 0.90. This ratio was also determined for sample II using distributions for the unannealed sample and for the sample annealed at 120°C for 9 h. In this case a value of 0.92 was found. There are a number of possible explanations why the values of this ratio is somewhat less than 1.0 for both samples. It may be due to experimental error; it may reflect a small increase in total length of all straight-chain segments for the annealed sample because there are fewer folds in the thickened crystal; or it may be due to the disappearance after annealing of certain conformations which can remove the contribution of some straight-chain segments[25]. However, the fact that the value of this ratio in two independent determinations approaches unity indicates that the sum of all these possible effects is small and that straight-chain length is essentially conserved. This result tends to confirm that the vibrational model employed is valid and that the spectroscopic measurements are quantitatively accurate.

Temperature dependence of f(L)

The temperature dependence of the LAM-1 band of a preannealed bulk-crystallized polyethylene has been investigated by Koenig and Tabb who used a laser line as an internal standard for comparing Raman scattering intensities[26]. They found that heating the sample below the crystallization temperature did not affect the band position but did cause a slight decrease in halfwidth and a large decrease in the band peak height after a temperature correction was made. When the sample was cooled to room temperature, the band regained its former shape and intensity, indicating that no significant morphological change had occurred as a result of the heating cycle. These authors interpreted the constancy in the band position to mean that there was no change in the average straight-chain length as a result of heating and hence no partial melting near the ends of the extended chains. The loss in intensity was attributed to the creation of 'defect chains' which undergo large-amplitude twisting motion about their long axis. They assumed such chains would not contribute or would contribute little to the intensity of the LAM-1 band. This explanation for the loss in intensity was clarified by Reneker and Fanconi[25] who showed through normal coordinate calculations that although the frequency and integrated intensity of LAM-1 is little affected by a smooth twist in a chain, the character and frequency of this mode is drastically changed by the presence of a localized conformational defect called a point dislocation. As a result, chains that contain a defect do not contribute to the intensity in the frequency region of the LAM-1 band.

We have remeasured the effect of temperature on LAM-1 since our intensity measurements are 'absolute' in the sense that they are independent of internal standards such as the intensity of a laser line[26] or another Raman band[27]. Sample III was annealed for 1.08 h at 129°C and its room-temperature spectrum measured. The sample was heated to 121° and 90°C, and spectra were measured at these temperatures. The sample was then cooled to room temperature and its spectrum remeasured. The spectra at room-temperature were identical within experimental error, indicating that no permanent changes had occurred in the sample as a result of heating.

The 25°, 90°, and 121°C spectra are shown in *Figure* 8. At higher temperatures, the intensity of the background increases while the intensity of the LAM-1 band decreases. As a result, it is difficult to draw a baseline for the 121°C spectrum. We were, however, able to derive from the 90°C spectrum the distribution of lengths that is shown in *Figure* 9 along with the room-temperature distribution. The distribution at 90°C is slightly broader and its value at the maximum is about 40 percent less than the distribution at 25°C.

Our results parallel those of Koenig and Tabb[26]. The peak position of the distribution is unchanged in going from 25° to 90°C although the peak height is reduced by about 40 percent. The reduction in intensity is attributed to the thermal generation of defects in the chain as first suggested by Reneker and Fanconi[25] on the basis of normal coordinate calculations for several conformations of a point dislocation in a fifty carbon atom normal alkane. This decrease in the intensity of the LAM-1 band is consistent with evidence for the thermal generation of defects from measurements of the intensity of rocking mode bands in 5 percent doubly deuterated polyethylene[28] as a function of temperature. The rocking mode bands in the range of 600 to 700 cm^{-1} were shown by normal coordinate analysis to provide a measure of the number of *trans–gauche* sequences present. Geometric constraints prohibit the generation of single *trans–gauche*

* These curves have been derived from the observed shape of LAM-1 uncorrected for effect of the natural shape. As a result, the distribution for the unannealed sample is somewhat broader than it would be if the true band shape were used (see previous discussion). However, only the integrated areas of the band are of interest, and their values are independent of the shape of the band

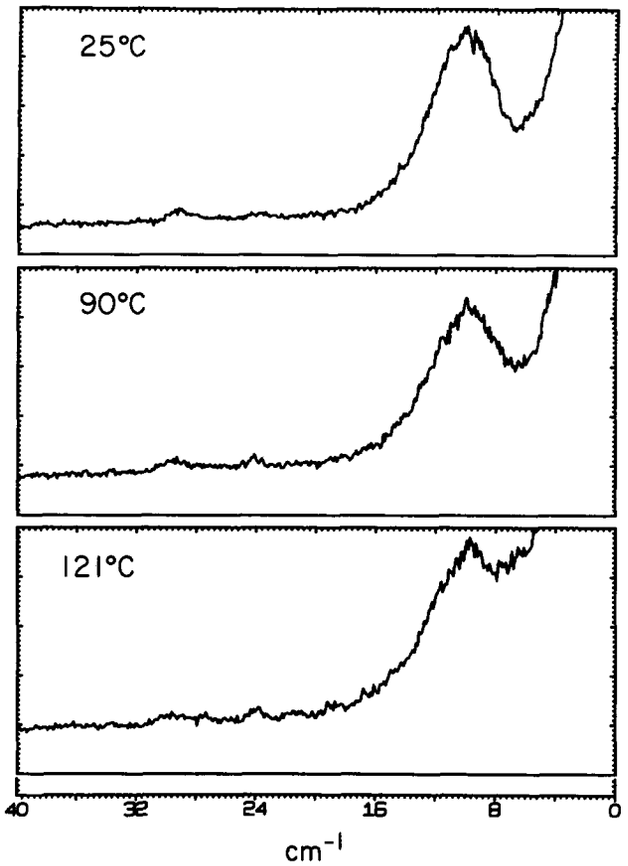

Figure 8 Temperature dependence of the low-frequency Raman spectra of preannealed (65 min at 129°C) sample III. Sample temperatures: 25°, 90°, and 121°C

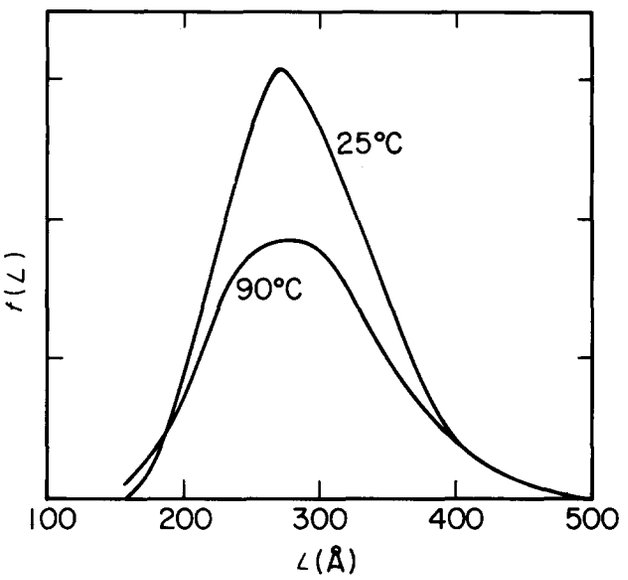

Figure 9 Temperature dependence of the distribution of straight-chain lengths based on the spectra shown in *Figure 8*

sequences at arbitrary locations in the crystal so the observed[28] increase in the number of *trans–gauche* sequences was taken as evidence for the thermal generation of point dislocations which contain several *trans–gauche* sequences.

Effect of annealing on f(L)

Relation between ν_{max} *and* $\Delta\nu_{\frac{1}{2}}$. The frequency of LAM-1 decreases with annealing. This behaviour, which has been reported earlier[26,29], is expected, since lamellar thickness is known to increase with annealing. The decrease in the frequency is accompanied by a change in the halfwidth of LAM-1. This change may be either positive or negative. For an unannealed solution-crystallized sample, annealing results first in a half-width increase, but continued annealing at higher temperatures eventually reverses this trend and causes the halfwidth to decrease.

Initially, the bandwidth of LAM-1 increases because of the increased breadth of the straight-chain length distribution. However, with higher annealing temperatures, a second factor comes into play which tends to narrow the band. Eventually this second factor dominates. As LAM-1 moves to lower frequencies, a unit on the frequency scale represents an ever increasing interval in the distribution of chain lengths. Thus below a certain frequency, there is a decrease in the observed halfwidth of the band even though the distribution itself continues to broaden as a result of the annealing.

There appears to be a general relation between the observed frequency ν_{max} and halfwidth $\Delta\nu_{\frac{1}{2}}$ of LAM-1 that is common to samples with the same initial morphology. This relation is shown in *Figure* 10 where ν_{max} is plotted against $\Delta\nu_{\frac{1}{2}}$ for a variety of polyethylenes. At frequencies below 12 cm^{-1}, the data for all samples tend to fall on a common curve. At higher frequencies, different samples appear to follow different curves depending on the initial morphological state although the curves have the same general form and show maxima when ν_{max} is near 20 cm^{-1}.

The form of curves in *Figure* 10 that relate $\Delta\nu_{\frac{1}{2}}$ and ν_{max} can be accounted for as follows. If $\Delta L_{\frac{1}{2}}$ for sample I is plotted against the reciprocal of L_{max}, these quantities being derived from the distribution curves of *Figure* 6, the nearly linear relation shown in *Figure* 11 is found. This relation may be written

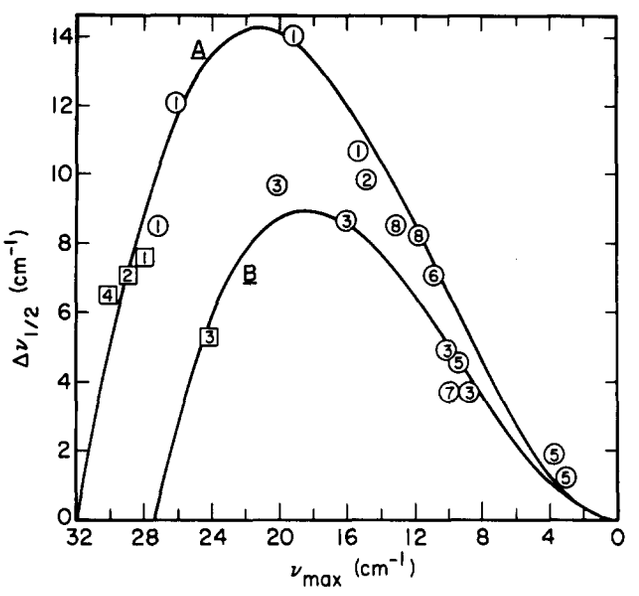

Figure 10 Observed band halfwidth $\Delta\nu_{1/2}$ (corrected for spectrometer slit width) *versus* peak frequency ν_{max} for LAM-1 of the following polyethylene samples: (1–3) solution-crystallized samples I, II, and III, respectively; (4) solution-crystallized; (5) bulk-crystallized; (6) extruded; (7) bulk-crystallized GREX Fraction B; (8) annealed drawn. Points □ designate unannealed solution-crystallized samples. Curves A and B were calculated using parameters based on data from samples I and III, respectively (see text)

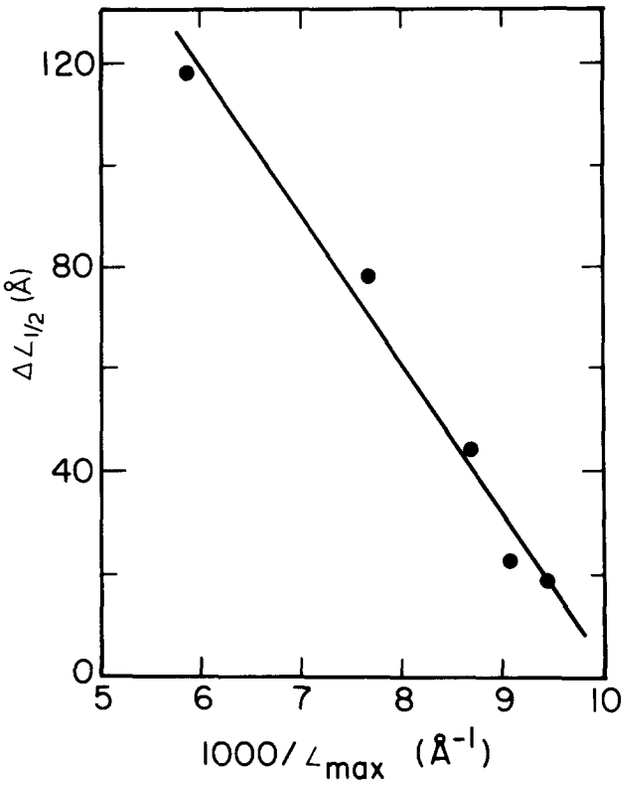

Figure 11 Halfwidth $\Delta L_{1/2}$ of the distribution of lengths of straight chains *versus* the reciprocal of the most likely length L_{max} (sample I)

$$\Delta L_{\frac{1}{2}} = c + d' L_{max}^{-1}. \quad (7)$$

Assuming that equation (7) is also valid for systems other than solution-crystallized samples and that L_{max}^{-1} is proportional to ν_{max} through equation (1), we may write

$$\Delta L_{\frac{1}{2}} = c + d\nu_{max} \quad (8)$$

where $d = d'/a$. Then from equation (1) we have the approximate relation

$$\Delta L_{\frac{1}{2}} = a\nu_{max}^{-2}\,\Delta\nu_{\frac{1}{2}} \quad (9)$$

where both $\Delta L_{\frac{1}{2}}$ and $\Delta\nu_{\frac{1}{2}}$ are defined as positive quantities. Combining equations (8) and (9) gives the LAM-1 band halfwidth in terms of ν_{max}

$$\Delta\nu_{\frac{1}{2}} = a^{-1}(c + d\nu_{max})\nu_{max}^2. \quad (10)$$

The maximum value of $\Delta\nu_{\frac{1}{2}}$ occurs at

$$\nu = -2c/3d. \quad (11)$$

Equation (10) was used to relate ν_{max} and $\Delta\nu_{\frac{1}{2}}$ for samples I and III. Values for c and d were derived from equation (8) and from the distribution curves. The calculated curves, A for sample I and B for sample III, are shown in *Figure* 10 along with the observed data points. For curve A, we used $c = 292$ Å and $d = -9.14$ (for L in angstroms and ν in wavenumber), and for curve B, $c = 247$ Å and $d = -8.96$. The frequency at which $\Delta\nu_{\frac{1}{2}}$ is a maximum for curve A as given in equation (10) is 21.3 cm^{-1}, very near the observed value of 21 cm^{-1}. We note that at frequencies less than 8 cm^{-1} the two curves give values for $\Delta\nu_{\frac{1}{2}}$ that differ from each other by less than 1 cm^{-1}.

Relation between L_{max} *and* $\Delta L_{\frac{1}{2}}$. Equation (7), plotted in *Figure* 12 for samples I and III, may be written

$$\Delta L_{\frac{1}{2}} = c(1 - c_2/L_{max}). \quad (12)$$

This equation is applicable, of course, only in the region where $L_{max} > c_2$. For values of L_{max} near c_2 (which corresponds to an unannealed sample), $\Delta L_{\frac{1}{2}}$ is near zero; for larger values of L_{max}, $\Delta L_{\frac{1}{2}}$ increases to a limiting value between 250 and 300 Å.

A useful quantity is the 'reduced halfwidth' $\Delta L_{\frac{1}{2}}/L_{max}$ equal to the distribution halfwidth divided by the most probable length. Highest order exists when $L_{max} = c_2$ or when $L_{max} = \infty$, in which case $\Delta L_{\frac{1}{2}}/L_{max} = 0$. Maximum disorder exists when $L_{max} = 2c_2$, i.e., when L_{max} assumes a value about twice its value for the solution-crystallized sample. For samples I and III, maximum disorder (by this definition) occurs when $L_{max} = 194$ and 224 Å, respectively. For these values, the reduced halfwidths equal 0.75 and 0.55.

In *Figure* 13, $\Delta L_{\frac{1}{2}}/L_{max}$ is plotted as a function of L_{max}. The two curves shown correspond to samples I and III and were calculated with the same parameters used to calculate curves A and B of *Figure* 10. Points representing experimentally determined values of the reduced halfwidth are included in *Figure* 13. Points 3 and 4 were derived from histograms of step heights measured on the surface of crystallized polyethylene as determined by electron microscopy[6,7]. Experimentally determined values derived from small-angle X-ray scattering measurements on unannealed solution-crystallized polyethylene[8,30] are also shown (points 1 and 2) and are found to fall near the calculated curves. On the other hand, the value of the reduced halfwidth for unannealed drawn polyethylene described in ref. 3 is anomalously high (point 5 on this Figure).

CONCLUSION

The distribution of lengths of straight-chain segments of solution-crystallized polyethylene was measured before

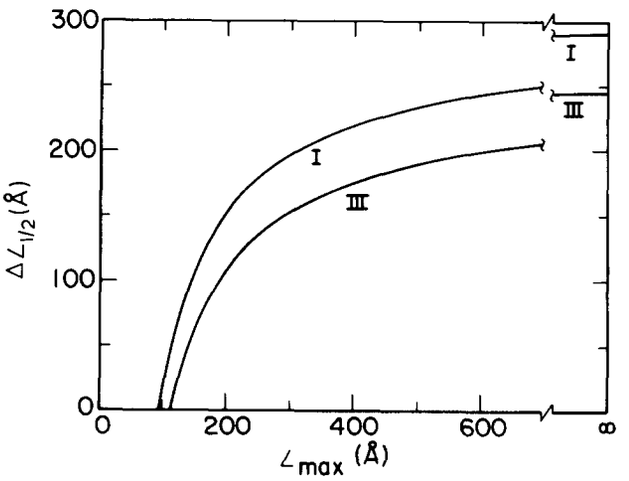

Figure 12 Halfwidth $\Delta L_{1/2}$ *versus* peak position L_{max} of the distribution curve for samples I and III calculated using equation (12) with parameters derived from curves A and B of *Figure 10*. Values of $\Delta L_{1/2}$ at $L_{max} = \infty$ are indicated

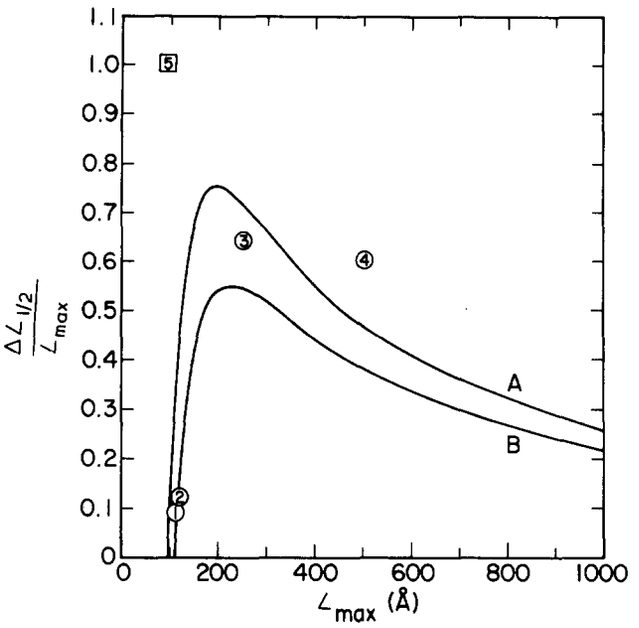

Figure 13 Reduced halfwidth $\Delta L_{1/2}/L_{max}$ *versus* L_{max}. Curves A and B were obtained using parameters derived from data on samples I and III, respectively. Numbered data points 1–4 are for equilibrium-crystallized samples: (1) and (2) are for unannealed solution-crystallized samples (estimated from SAXS studies described in refs. 8 and 3, respectively); (3) and (4) are for melt-crystallized samples (estimated from electron microscopic investigations described in refs. 6 and 7, respectively). The numbered datum point 5 is for a nonequilibrium-crystallized sample: unannealed drawn polyethylene (determined from a Raman study described in ref. 3)

annealing and then remeasured each time after *in situ* annealing at successively higher tempeatures. The halfwidth of the distribution was about 12 to 14 Å for the unannealed sample. The halfwidth increased with increasing annealing temperatures and at 120°C reached a value about 10 times that of the original sample. Integrated intensity measurements indicate that the annealing did not significantly change the total length of straight-chain segments. Increases in temperature reduced the intensity of the LAM-1 band, as would be expected from the thermal generation of defects.

The distribution halfwidth $\Delta L_{\frac{1}{2}}$ and the most probable length L_{max} were found to be related over the range of annealing temperatures used in this study by

$$\Delta L_{\frac{1}{2}} = c(1 - c_2/L_{max})$$

The values of c and c_2 are equal to about 270 and 105 Å respectively. This relation implies that for long annealing times, and hence large L_{max}, the halfwidth $\Delta L_{\frac{1}{2}}$ approaches a limiting value near 300 Å. Raman measurements in PE samples for which $L_{max} > 500$ Å support the idea of a limiting value for the distribution halfwidth[31].

ACKNOWLEDGEMENTS

We would like to thank Dr John F. Rabolt for checking some of our n-alkane bandwidths with independent measurements. We are also indebted to Dr G. Thomas Davis for supplying us with a sample of 'GREX Fraction B' polyethylene. Dr Bruno Franconi and Dr F. A. Khoury supplied useful information and made helpful suggestions.

REFERENCES

1 Sadler, D. M. and Keller, A. *Science* 1979, **203**, 263
2 Snyder, R. G., Krause, S. J. and Scherer, J. R. *J. Polym. Sci. Polym. Phys. Edn.* 1978, **16**, 1593
3 Snyder, R. G., Scherer, J. R. and Peterlin, A. *Macromolecules* 1981, **14**, 77
4 Schaufele, R. F. and Shimanouchi, T. *J. Chem. Phys.* 1967, **47**, 3605
5 Rabolt, J. F. and Fanconi, B. *J. Polym. Sci., Polym. Lett Edn.* 1977, **15**, 121; Rabolt, J. F. and Fanconi, B. *Polymer* 1977, **18**, 1258; Hsu, S. L., Krimm, S., Krause, S. and Yeh, S. Y. *J. Polym. Sci. Polym. Lett. Edn.* 1976, **14**, 195
6 McHugh, A. J. and Schultz, J. M. *Phil. Mag.* 1971, **24**, 155
7 Bassett, D. C. and Phillips, J. M. *Polymer* 1971, **12**, 730
8 Crist, B. and Morosoff, N. *J. Polym. Sci. Polym. Phys. Edn.* 1973, **11**, 1023
9 Windle, A. H. *J. Mater. Sci.* 1975, **10**, 252
10 Windle, A. H. *J. Mater. Sci.* 1975, **10**, 1959
11 Weeks, J. J. *J. Res. Natl. Bur. Stand., Sect. A* 1963, **67**, 441
12 Sadler, D. M., Williams, T., Keller, A. and Ward, I. M. *J. Polym. Sci. A-2* 1969, **7**, 1819
13 Keller, A., Martuscelli, E., Priest, D. J. and Udagawa, Y. *J. Polym. Sci. A-2* 1971, **9**, 1807
14 Snyder, R. G. and Scherer, J. R. *J. Polym. Sci. Polym. Phys. Edn.* 1980, **18**, 421
15 Hartwig, C. M., Wiener, E. and Porto, S. P. S. *Bull. Am. Phys. Soc.* 1970, **15**, 327; Devlin, G. E., Davis, J. L., Chase, L. and Geschwind, S. *Appl. Phys. Lett.* 1971, **19**, 138
16 Scherer, J. R. *Appl. Opt.* 1978, **17**, 1621
17 Blundell, D. J., Keller, A. and Kovacs, A. J. *J. Polym. Sci. B* 1966, **4**, 481
18 Geil, P. H. 'Polymer Single Crystals', R. E. Krieger, New York, 1973
19 Keller, A. *Rep. Prog. Phys.* 1968, **31**, 623
20 Khoury, F., Fanconi, B., Barnes, J. D. and Bolz, L. H. *J. Chem. Phys.* 1973, **59**, 5849
21 Seshadri, K. S. and Jones, R. N. *Spectrochim. Acta* 1963, **19**, 1013
22 Placzek, G. 'Marx Handbuch der Radiologie' 2nd Ed., Vol. 6, Part 2, p. 209, Acad. Verlagsges, Leipzig, 1934
23 Dijkman, F. G. and Van der Mass, J. H. *Appl. Spectrosc.* 1976, **30**, 545
24 Rabolt, J. IBM Research Laboratories, private communication
25 Reneker, D. H. and Fanconi, B. *J. Appl. Phys.* 1975, **46**, 4144
26 Koenig, J. L. and Tabb, D. L. *J. Macromol. Sci. Phys.* 1974, **9**, 141
27 Strobl, G. R. and Eckel, R. *Colloid Polym. Sci.* 1980, **258**, 570
28 Reneker, D. H., Mazur, J., Colson, J. P. and Snyder, R. G. *J. Appl. Phys.* 1980, **51**, 10
29 Peticolas, W. L., Hibler, G. W., Lippert, J. L., Peterlin, A. and Olf, H. *Appl. Phys. Lett.* 1971, **18**, 87
30 Strobl, G. R. *J. Appl. Crystallogr.* 1973, **6**, 365
31 Snyder, R. G. *J. Polym. Sci. Polym. Phys. Edn.* in press